

Submicron Nanoporous Polyacrylamide Beads with Tunable Size for Verapamil Imprinting

Ali Nematollahzadeh, Mohammad J. Abdekhodaie, Akbar Shojaei

Department of Chemical and Petroleum Engineering, Sharif University of Technology, P. O. Box 11155-9465, Tehran, Iran

Received 9 January 2011; accepted 4 August 2011

DOI 10.1002/app.35426

Published online 17 December 2011 in Wiley Online Library (wileyonlinelibrary.com).

ABSTRACT: Submicron sized polyacrylamide particles were prepared via modified precipitation polymerization method. Experimental design based on Taguchi approach was employed to study the influence of the polymerization composition including monomer (acrylamide), crosslinker (methylenebisacrylamide), initiator (azobisisobutyronitrile), and modifier (polyvinylpyrrolidone, K-30), on the size and morphology of the particles. Varying the polymerization composition, submicron-particles with sizes ranging between 100 and 600 nm were achieved. In all the cases, polydispersity index (PDI) of the particle size was found to be almost 1 indicating uniformity of the particle size. The concentration of crosslinker was found to be the most influential parameter on the particles size and the modifier concentration as an extra tunable parameter was believed

to affect the nucleation mechanism and the viscosity of the medium to help controlling the particle size. To validate the optimization, particles with a preset diameter, i.e., 500 nm, were synthesized based on the composition predicted by the mathematical correlation. The polymer with the preset particle size was also imprinted with verapamil and characterized by FTIR, DSC, SEM, physisorption, elemental analysis, swelling, and batch rebinding experiments. The verapamil imprinted polymers bearing nano-cavities exhibited high affinity with imprinting factor 2.17 towards the target molecule. © 2011 Wiley Periodicals, Inc. *J Appl Polym Sci* 125: 189–199, 2012

Key words: submicrobeads; nanoporous; precipitation polymerization; verapamil imprinted polymer; Taguchi method

INTRODUCTION

Polymeric microbeads have long been used in many areas including ion exchange resins and sorbents, catalyst supports, materials for biomedical applications, and stationary phases for high performance liquid chromatography (HPLC).¹ In such applications, it is of prime concern to obtain beads with an appropriate particle size and morphology. For example, particles smaller than 450 nm are not suitable for HPLC separation column, because it may cause severe problems in the system, such as clogging the column and the frits.² On the contrary, to obtain a system with high adsorption capacity, small and/or porous particles are required. In short, for a special application there is a need for a specific particle size and morphology.

Polymeric microbeads of a particular size and uniformity are generally obtained with one of the heterogeneous polymerization methods such as suspension,³ inverse-phase suspension,³ emulsion,⁴ dispersion,⁵

precipitation,⁶ and multistep-swelling⁷ polymerization. In such methods, molecular imprinting technique could be easily integrated to produce specific molecular recognition sites for a target molecule.

Molecular imprinting involves the arrangement of functional monomers around template molecules in a porogenic solvent. The complex is subsequently copolymerized with a suitable crosslinker through free radical polymerization mechanism. After the removal of the template, the specific cavities, which are complementary in shape, size, and chemical functionality to the template, are left within the polymer matrix. These specific cavities can selectively rebind target (i.e., the template) molecule. Typically, molecularly imprinted polymers (MIPs) were prepared by a bulk polymerization method. Preparation of MIPs via the conventional bulk polymerization method always leads to monolithic materials which have to be pulverized, crushed, and sieved to produce polymer particles with a desired size.^{8,9} This method always results in particles with irregular shapes and size. Additionally, during the crushing and sieving processes large quantities of the material and also recognition sites are destroyed, and typically less than 50% of the ground polymer is recovered as useable particles.^{10,11} This causes a system with low capacity and slow mass transfer properties leading to the reduction of system efficiency.

Correspondence to: M. J. Abdekhodaie (abdmj@sharif.edu).

Contract grant sponsor: Sharif University of Technology (Tehran, Iran).

Among the aforementioned polymerization methods, precipitation polymerization as an attractive stabilizer-free method produces particles in the range of 0.1–10 μm , which involves polymerization of monomers in diluted solution.¹² In this method, the special mechanism of the reaction obviates the need for stirrer and stabilizer.¹³ Besides precipitation polymerization, dispersion polymerization has been used to make spherical MIPs. In dispersion polymerization method, the initial state of the reaction is the same as that in precipitation polymerization, but the formed droplets needs to be stabilized by a stabilizer or a surfactant. The method produces polymer particles within ranges from about 1–10 μm .¹²

Horváth et al.¹⁴ prepared micron size polymer microspheres using a modified precipitation polymerization method. They studied the effect of addition of paraffin oil in the polymerization solution on the morphology of the particles. However, they did not study the influence of different parameters on the particle size. In our previous work,¹⁵ we produced hierarchically structured porous polymer particles with predefined particle size and pore properties for protein imprinting. In the present work, establishing a modified precipitation polymerization technique submicron sized molecularly imprinted particles was produced to target verapamil as template. Verapamil is an L-type calcium channel blocker of the phenylalkylamine class which has been used as a vasodilator during cryopreservation of blood vessels, and also in the treatment of cluster headaches, hypertension, and angina pectoris.¹⁶ The measurement and identification of an active pharmaceutical ingredient (API) like verapamil is addressed using several different techniques in a series of analyses. The techniques are often a time consuming and laborious process. However, the verapamil imprinted polymer can be used in drug purification or detection.¹⁷ The literature shows a few reports on the verapamil imprinted polymers. Mullet et al.¹⁷ presented verapamil imprinted polymethacrylic acid via the bulk polymerization of methacrylic acid (MAA) and ethylene glycol dimethacrylate (EDMA) to investigate the verapamil metabolism and to further evaluate the application of the polymer in solid-phase extraction. Employing precipitation polymerization method, Javanbakht et al.¹⁸ reported verapamil imprinted polymers produced by the same recipe as Ref. 17 for selective solid-phase extraction of verapamil from biological fluids and human urine. However, they did not investigate the influence of different parameters neither on the particle size nor on the polymer morphology. The present work is, therefore, a detailed investigation on the size of polymer particles produced by the modified precipitation polymerization. The method is a unique hybrid of precipitation and

dispersion polymerization in which we take advantage of both methods to control the particle size. For the experimental proof of the concept, acrylamide was copolymerized with methylenebisacrylaide to prepare the submicron sized non-imprinted polymer (NIP) particles. In order to reduce the number of experiments and to determine the most influential parameters on the particle size and possible interaction between the parameters (considering the influence of system composition including monomer, crosslinker, initiator, and modifier), experimental design based on Taguchi approach¹⁹ was employed. Composition of the NIP for a specified particle size which already was predicted by the Taguchi analysis was selected to prepare the corresponding MIP. Verapamil rebinding and pore properties of the obtained submicroparticle MIP/NIP were investigated.

EXPERIMENTAL

Materials

Verapamil-HCl (2-(3,4-dimethoxyphenyl)-5-[[2-(3,4-dimethoxyphenyl)ethyl] (methyl)amino]-2-isopropylpentanenitrile) was purchased from Sigma-Aldrich (St. Louis, MO). Analytical grades of acrylamide (AAm) and *N,N'*-methylenebisacrylamide (MBA) were purchased from Merck (Darmstadt, Germany) and double-recrystallized in methanol and acetone, respectively. 2,2'-Azobis (2-isobutyronitrile) (AIBN) was obtained from Merck and recrystallized in methanol as well. Polyvinyl pyrrolidone (PVP-K30), acetonitrile (MeCN), dimethylsulfoxide (DMSO), methanol, and acetic acid provided by Merck were used as received.

Taguchi analysis

In an experiment that multiple factors affect the result, design of experiment helps defining and investigating all possible conditions. Taguchi approach is one of the common methods to perform the design of experiments. The technique is applied in four steps: (1) choosing the design parameters or the most influential factors and levels for each factor, (2) randomly distributing the runs (experiments) in a special set of orthogonal arrays (OA) and collecting the result of each set of experiment, (3) analyzing the results to estimate the contribution of individual factor (in this step the analysis of variance (ANOVA) is performed to determine the percent contribution of each factor. Study of the ANOVA results helps to decide which of the factors need control and which do not), and (4) running a confirmatory tests using the optimum condition achieved in step 3.

TABLE I
Different Factors and Their Levels for Design of Preparation of NIP

Factors	Levels			
	1	2	3	4
(A) Monomer, AAm (wt %) ^a	0.25	0.5	0.75	1
(B) Crosslinker, MBA (wt %) ^a	1	2	3	4
(C) Initiator, AIBN (wt %) ^b	1	2	3	4
(D) Modifier, PVP (wt %) ^a	0	0.5	1	1.5

^a Based on total solvent amount of 25 mL.

^b Based on total amount of monomers.

The factors used in this study include the concentrations of monomer, crosslinker, initiator, and modifier each at four levels. Table I describes the factors and their levels. In this table, the weight percent of the monomers (AAm and MBA) are based on the total volume of the solvent while the weight percent of the initiator (AIBN) is based on the total mass of the monomers. For an experiment with four factors each at four levels, Taguchi's method suggests an M_{16} OA.¹⁹ Table II shows the standard M_{16} orthogonal array. In this table, each row, which is indicated by a number, shows a trial condition and each column represents the various levels of a factor. The statistical analysis relevant to this OA including average trend of influence and the relative influence of factors (referred to as contribution of factor) on the results was conducted using Minitab (V15.1) and Qualitek-4 software.

Furthermore, the extent of interaction between any factor pairs, in terms of the severity index (SI) in percent ranging between 0 and 100%, was displayed in a histogram format. The SI value of 100% indicates the strongest interaction between two factors, while 0% SI shows no interaction.

Preparation of the particles

The polymer particles (16 samples, P1–P16) were prepared according to the composition given in Table II. Typically, in a glass vial, AAm, MBA, and PVP were dissolved in 0.5 mL DMSO. The mixture was shaken for 5 min and then 24.5 mL MeCN and AIBN were added to the mixture. Then the vial content was sparged with nitrogen for 10 min in an ice bath. The polymerization was thermally initiated at 60°C in an oven (JP Selecta, TV), capable of maintaining the preset temperature within $\pm 1^\circ\text{C}$ and circulating hot air (with a homemade circulator). The reaction duration was at least 16 h to let the polymerization to be completed.

To produce MIP, in a glass vial, AAm (0.447%, 111.7 mg or 1.6 mmol) was dissolved in 0.5 mL DMSO and then verapamil (200 mg, 0.4 mmol) was

added to the mixture. To provide a complex between the template and the monomer, the mixture was stirred for 16 h. Later, MBA (4%, 1.00 g or 6.5 mmol) and PVP (0.469%, 117.4 mg or ~ 0.003 mmol) and then 24.5 mL MeCN and 0.14 mmol AIBN were added to the mixture. The rationale for the selection of these amounts is discussed in Result and Discussion section. After addition of AIBN, the vial content was sparged with nitrogen for 10 min in an ice bath. The polymerization solution was polymerized in the same manner as mentioned above. At the end of the reaction, the particles were separated from the reaction medium using centrifugation (EBA20, Hettich). NIP was prepared in the same manner without addition of the template molecule. The resultant products (MIP/NIP) were washed with methanol and acetic acid (9 : 1, v/v) and then with methanol to remove the template, modifier, and any unreacted monomers or oligomers. The removal of the template was confirmed by UV spectroscopy of extraction solvent at a wavelength of 280 nm. The samples were dried in a vacuum oven at 40°C overnight.

Particle morphology and size

The morphology of the synthesized particles was assessed by scanning electron microscope (SEM, LEO 1455 VP, Oxford). Final images were recorded from randomly chosen areas at magnification indicated in each SEM. The number of polymer particles (in total 50 particles for each sample) could be counted via ImageJ software²⁰ from the scanning electron micrographs. The statistical characteristics of particles namely number-average diameter (D_n),

TABLE II
Experimental Layouts of M_{16} Orthogonal Array

Run no.	Factor levels ^a			
	A	B	C	D
P1	1	1	1	1
P2	1	2	2	2
P3	1	3	3	3
P4	1	4	4	4
P5	2	1	2	3
P6	2	2	1	4
P7	2	3	4	1
P8	2	4	3	2
P9	3	1	3	4
P10	3	2	4	3
P11	3	3	1	2
P12	3	4	2	1
P13	4	1	4	2
P14	4	2	3	1
P15	4	3	2	4
P16	4	4	1	3

^a The value of the levels are given in Table I.

weight-average diameter (D_w), and polydispersity index (PDI), were calculated using the following equations^{21,22}:

$$D_n = \frac{\sum d_i}{n} \quad (1)$$

$$D_w = \frac{\sum (d_i)^4}{\sum (d_i)^3} \quad (2)$$

$$\text{PDI} = \frac{D_w}{D_n} \quad (3)$$

where d_i represents the diameters of the microspheres, and n is the number of particles. Particle size was rounded up to ± 1 nm.

Rheological measurement

The viscosity of the polymerization medium (MeCN) at different concentrations of PVP (0.25, 0.5, 0.75, 1, 1.25, 1.5%) was measured using Brookfield viscometer (Model DV-E viscometer). The removable sample chamber (equipped with temperature probe) was filled with about 16 mL of each sample and the measurements were conducted at 25°C or 60°C.

FTIR and UV/vis spectroscopy

Fourier transforms infrared spectroscopy (FTIR) was used to study the polymer structure and to define extraction of the template and the modifier from the samples. Samples were accurately weighed in which the mass ratio of sample : KBr was 1 : 20 and infrared spectra were carried out by using 32 scans for each sample with a resolution factor of 4. Infrared spectra were recorded in the wave-number range of 4000–450 cm^{-1} on an ABB Bomem MB series spectrophotometer. Ultraviolet spectra were collected on Lightwave UV/vis spectrophotometer S2000 series.

Elemental analysis

Analyses for carbon, hydrogen, and nitrogen were performed using a Heraeus Elemental Analyzer CHN-O-Rapid (Elemental-Analyses system, GmbH). About 10 mg of dried sample was submitted to elemental analysis. The experimental values obtained in this way were compared with the theoretical values calculated through eq. (4) given as follows:

$$\%X = M_X \left(\frac{\sum_{j=1}^k N_{j,X} \cdot n_j}{\sum_{j=1}^k n_j M_j} \right) \times 100 \quad (4)$$

where, X displays the C, H, or N element and $N_{j,X}$ is the number of the element X in compound j

(monomer or crosslinker). M_X and M_j are the molecular weight of the element X and compound j respectively, and n_j is the mole percent of the compound j . For a system with two monomers $k = 2$.

Thermal analysis

Thermal analysis was carried out by means of a Perkin–Elmer differential scanning calorimeter (DSC) consisting of thermal analysis microprocessor controller. Temperatures and enthalpies were calibrated using indium phase transition (99.99% pure; heat of fusion, 28.45 J/g; melting point, 429.76 K). Samples (5.0 mg) were weighed by a balance with accuracy of 0.1 mg and encapsulated in aluminum crimped pans. Thermal curves were recorded with a heating rate of 10 °C/min in a temperature range from 25 to 190°C under a dry nitrogen purge (20 cm^3/min). Before each scan, a baseline was recorded with the same heating rate and then subtracted from the experimental scan.

Surface area and pore size analysis

The pore properties of the samples including surface area, pore volume, and pore size were assessed by nitrogen gas sorption analyzer (NOVA-4000e, Quantachrome), and were determined by a Multipoint BET (Brunauer–Emmett–Teller) method. The BJH (Barret–Joyner–Halenda) method was applied to calculate the pore size distribution from the analysis of the desorption branches of the isotherms. Before the experiment, a total of 100 mg of the polymers were degassed at 40°C for 17 h. The dry polymer was used for nitrogen sorption isotherms at -196°C . The average pore diameter was calculated using the Wheeling equation expressed as²³:

$$P_d(\text{nm}) = 4 \times 10^3 \frac{\text{Pore volume (cc/g)}}{\text{Surface area (m}^2/\text{g)}} \quad (5)$$

Swelling ratio

In order to better elucidate the difference between the dry and swollen state of the polymers, swelling tests were performed in acetonitrile. Swelling was measured in graduated NMR tube by allowing a known volume and weight of dry polymer to equilibrate in acetonitrile, where after the volume of the swollen particles was measured. The swelling ratio, given as volume of the swollen polymer to volume of dry polymer, was read after 24 h.

Batch binding experiment

One hundred milligrams of each MIP and NIP polymer particles were placed in a separate HPLC glass

vials containing 1 mL of a 10 mM verapamil standard solution prepared in MeCN. Each suspension was gently shaken for 24 h and then the supernatants were separated by centrifuge. The concentration of verapamil in the supernatants solution was measured by UV spectroscopy at a wavelength of 280 nm.

RESULTS AND DISCUSSION

It is known that the concentrations of the components involved in the polymerization are the key parameters in the synthesis of the MIPs and the particles.^{12,24} Therefore, in the design of the experiments, the levels for each factor was chosen, taken into account the common molar ratios between template : monomer : cross-linker which corresponds to 1 : 4 : 20 (i.e., 83 mol% crosslinker over total monomers).²⁴ It is noteworthy to mention that in this study the molar ratio was 1 : 4 : 16 (or 80 mol% crosslinker over total monomers), which is close to the common molar ratio. We slightly decreased the amount of the crosslinker to help the slightly big template penetration into the nanocavities.²⁵ The chosen monomers should be soluble easily in the solvent used in the addition to bear the highest interactions with the template. Moreover, in the molecular imprinting technology, the best imprinting porogens are solvents with very low dielectric constant such as toluene, chloroform, acetonitrile, etc. The use of more polar solvents will weaken the interaction forces resulting in poorer recognition. Thus the solvent must be chosen carefully to maximize the possibility of the formation of template-functional monomer complex.²⁶ Therefore, in this work acetonitrile was used as the porogenic solvent. Since MBA at room temperature is not soluble in acetonitrile, a small quantity of DMSO (0.5 mL or 2%) was used as co-solvent. Spizzirri and Peppas²⁷ proofed that DMSO as an amphipathic solvent does not take part in the hydrogen bond host-guest interaction but it helps in the achievement of porous materials. According to literature, the volume ratio of the monomer phase to the polymerization medium was kept within 1–5%.⁶

Taguchi analysis of the particles size

Influence of the composition of polymerization system on the particles size characteristics for a set of experiments defined using OA (M_{16}) is presented in Table III. The results indicate that the particles obtained from each experimental run are in submicron size, i.e., diameters less than 1 μm . It is also deduced that the PDI of the particles is close to 1 showing the uniform size of the particles obtained in all the cases. The smallest particle size belongs to

TABLE III
Average Particle Size (nm) and Polydispersity Index for the 16 Samples Prepared Based on M_{16} (OA)

Sample	D_n (CV%) ^a	D_w (CV%) ^{a,b}	PDI (CV%) ^{a,b}
P1	191 (1.83)	194 (1.30)	1.02 (2.20)
P2	239 (2.51)	258 (1.89)	1.08 (2.91)
P3	402 (1.47)	408 (0.98)	1.01 (1.75)
P4	511 (1.27)	529 (1.10)	1.04 (1.62)
P5	130 (5.23)	136 (4.21)	1.05 (6.39)
P6	138 (4.86)	141 (3.96)	1.02 (6.14)
P7	602 (1.10)	626 (0.88)	1.04 (1.35)
P8	534 (1.05)	547 (0.75)	1.02 (1.23)
P9	157 (2.68)	163 (2.11)	1.04 (3.28)
P10	372 (0.75)	376 (0.23)	1.01 (0.78)
P11	273 (2.53)	285 (1.97)	1.04 (3.08)
P12	541 (1.18)	555 (0.84)	1.03 (1.41)
P13	176 (2.05)	185 (1.68)	1.05 (2.52)
P14	371 (1.81)	386 (1.12)	1.04 (2.04)
P15	245 (0.94)	281 (0.72)	1.15 (1.03)
P16	249 (1.89)	271 (0.99)	1.09 (1.96)

^a Coefficient of variation (CV% = Standard deviation \times 100/mean).

^b The total standard deviation was calculated employing multiplication and division rule for standard deviations.

experiment P5 (D_w of 136 nm) and the biggest one is relevant to experiment P7 (D_w of 626 nm). This indicates that the domain of variation of particles size by changing the content of constituents is noticeable (more than fourfold increase in the average particle size).

The data relevant to the particle size, according to Table III, were used to perform the analysis of variance (ANOVA) using Qualitek-4 software. The results are represented in Table IV. The presented results indicate that the crosslinker has the biggest impact on the particles size (Percent $P \approx 52\%$). The initiator has the second order in influencing the particle size (Percent $P \approx 24\%$), the role of monomer concentration on the particle size is found to be very little. Figure 1 shows the effect of the factors on the weight average particle size with the levels variation. Obviously, the concentrations of initiator and crosslinker (two most influential parameters) display increasing trend on the average particle size. Indeed, the initiator concentration alters the particles size from 200 nm to 380 nm (difference of 180 nm), while the crosslinker concentration alters the particles size in a wider range between 163 nm and 459 nm (difference of 296 nm). This may be attributed to the entropic precipitation mechanism of the polymerization in which the cross linker prevents the polymer and solvent from freely mixing.²⁸ Unlike the conventional dispersion polymerization, in the absence of any modifier (or stabilizer), the beads were still stable and it was believed that they were formed through precipitation polymerization mechanism. Additionally, through Figure 1 and Table III, it was found that as the amount of the modifier increases the particle size decreases. This can be due to the fact

TABLE IV
Analysis of Variance (ANOVA) for Particle Size Obtained by Qualitek-4 (Quality Characteristic (QC) = Smaller is Better)

Factors	DOF ^a (<i>f</i>)	Sum of sqrs ^b (<i>S</i>)	Variance ^c (<i>V</i>)	F-ratio ^d (<i>F</i>)	Pure sum ^e (<i>S'</i>)	Percent P ^f (%)
Monomer	3	18,926	6309	102.2	18741	4.98
Crosslinker	3	197,461	65,820	1066	197,275	52.39
Initiator	3	912,92	30,431	493	91,107	24.19
Modifier	3	68,694	22,898	371	68,509	18.19
Other/Error	3	185	62			0.25
Total	15	376558				100.00%

^a Degree of freedom, is the number of independent quantities that can be calculated from experimental data and cannot exceed the number of data points applied to characterize four separate items.

^b Sum of squares, is calculated by adding deviations of the individual data from the mean value (\bar{Y}), $S_T = \sum_{i=1}^N Y_i^2 - \frac{T^2}{N}$; where, T is the summation of the all results and N is the number of the experiments.

^c Variance (or mean squares): $V_A = \frac{S_A}{f_A}$.

^d F-ratio: $F_A = \frac{V_A}{V_e}$.

^e Pure sum of squares: $S'_A = S_A - (V_e f_A)$.

^f Percent influence: $P_A = \frac{S'_A}{S_T}$, where V_e is the variance for the error term (obtained by calculating error sum of squares and dividing by error degrees of freedom) and f_A is the degrees of freedom (DOFs) of factor A .

that when the concentration of the modifier increases, the number of nuclei of particles increases. Indeed, in the absence of any modifier, the initially formed polymer nuclei are adhered together as a result of collision and in a certain size (or weight) they start precipitating.¹² Moreover, it has been reported¹² that the viscosity of the reaction medium may influence the particle size in a way that increasing the viscosity of the polymerization medium decreases the particle size. In other word, increased viscosity, opposing the motion of the particles relative to its neighbors,²⁹ results in smaller particles. Hence, viscosity of the reaction medium (v_m) and modifier concentration (C_s) can affect the average particle size (\bar{d}) inversely, according to the following expression,¹² but with the two above mentioned mechanisms.

$$\bar{d} \equiv f\left(\frac{1}{v_m \cdot C_s}\right) \quad (6)$$

In this work, viscosity of the reaction medium was found to be a linear function of the modifier (PVP)

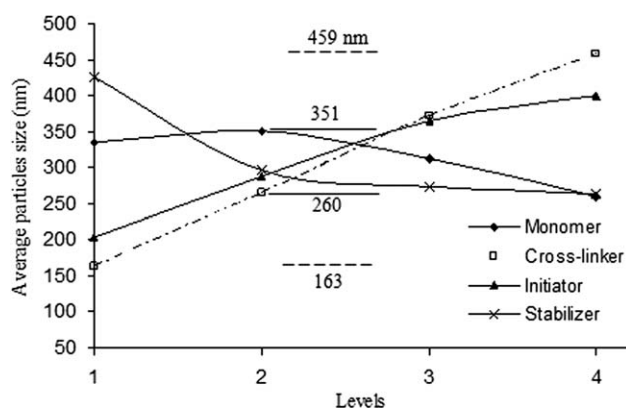
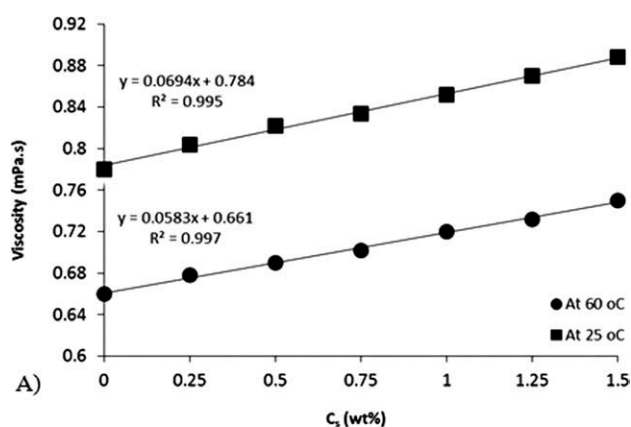


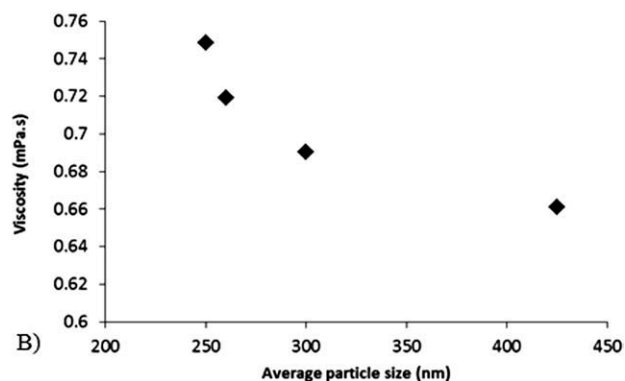
Figure 1 Main effect plot of average particle size.

concentration [Fig. 2(A)], which could be estimated by the following equation at 60°C:

$$v_m = 0.0583C_s + 0.661; (R^2 = 0.997) \quad (7)$$



A)



B)

Figure 2 A: Viscosity change of the polymerization medium (MeCN+PVP) versus the concentration of the modifier (PVP-K30) at two different temperatures (25°C and 60°C) and (B) Effect of polymerization medium viscosity (at 60°C) on average particle size.

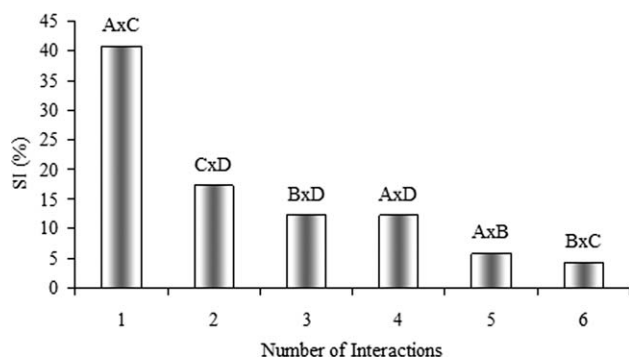


Figure 3 Interacting factor pairs (in order of SI): (A) monomer, (B) crosslinker, (C) initiator, (D) modifier.

where v_m is the viscosity of the solution (mPa s) and C_s is the concentration of the modifier (wt %). The effect of polymerization medium (MeCN + PVP) viscosity on the average particle size is shown in Figure 2(B). This correlation indicates that the viscosity of the reaction medium increases slightly by addition of the modifier. Therefore, the reduction of the particle size with the modifier concentration is speculated to be much prominent to the nucleating role of the modifier (not to the enhanced viscosity).

Furthermore, an analyzed possible interaction between the four factors, the six possible interacting factor pairs ($4 \times (4 - 1)/2 = 6$) in order of the interaction severity (SI), is represented in Figure 3, quantitatively. It was observed that the interaction between the monomer and initiator (A \times C) is more severe than the other interactions.

Figure 4 displays the particle morphology of typical systems in the presence (samples P1 and P14) and absence of the modifier (sample P4).

Correlation of particle size and the polymerization composition

Due to the influence of the different parameters on the particle size, a nonlinear model is required to describe the correlations between the components of the reaction and the mean particle size. Following previous studies,^{30,31} contour plot between any pairs of compo-

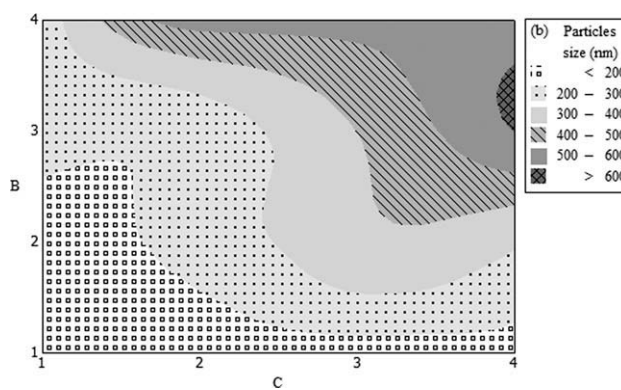


Figure 5 Contour plot of crosslinker (B) vs. initiator (C).

nents with respect to the particles size (see Fig. 5) by means of Akima's polynomial expressed as eq. (8). Akima's polynomial is a very useful technique for the estimation of the optimal curve.³² Moreover, it is noteworthy to point out that the two dimensional interpolation (Akima's method) can be addressed as a fast calculation or smoothing method.

$$d_p = \sum_{i=0}^5 \sum_{j=0}^{5-i} \alpha_{ij} C^i B^j \quad (8)$$

where α_{ij} are the coefficients of each local polygon, B and C are coordinate distances relative to some local origin (typically the crosslinker and initiator concentrations), and i and j are dummy variables. Although the contour plot of the other factors could also be obtained easily, the contour plot of crosslinker and initiator is presented here due to their biggest impact on the particle size (see Fig. 1 and Table IV). Obviously, with an increase in the concentrations of both crosslinker and initiator, bigger particles can be obtained.

Furthermore, in order to confirm the optimization results (i.e., step four in Taguchi method: running a confirmatory tests using the optimum condition), the optimum condition for a target value of 500 nm with a weight factor of 5.0 and importance value of 5.0 (the values that emphasize on the objective) is given in Figure 6. This has been performed by the

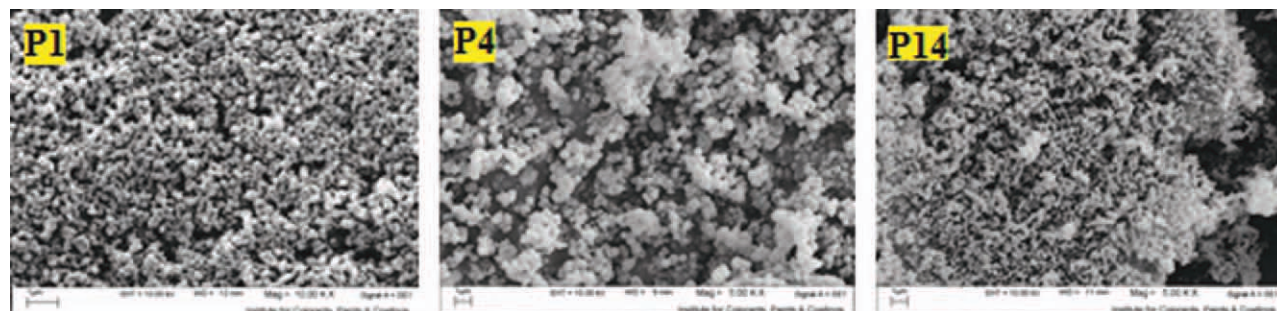


Figure 4 SEM image of sample P1, P4, and P14. [Color figure can be viewed in the online issue, which is available at wileyonlinelibrary.com.]

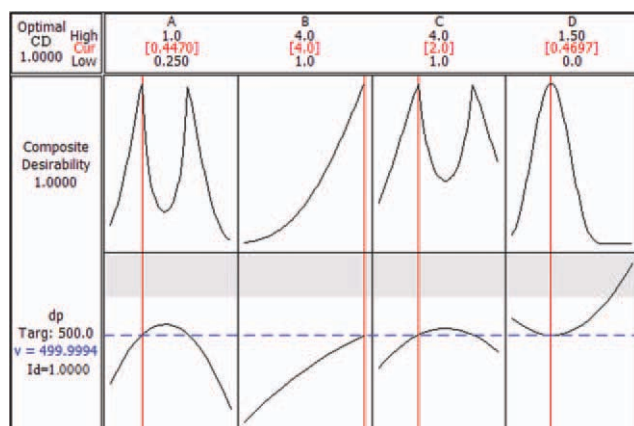


Figure 6 Minitab optimization plot to target 500 nm particles. CD: composite desirability; Id: individual desirability; High: highest parameter values; Low: lowest parameter values; Cur: current or optimum values; and (A–D) are defined in Table I. [Color figure can be viewed in the online issue, which is available at wileyonlinelibrary.com.]

Minitab software. To obtain particles with the average diameter of 500 nm, the optimum concentrations for the components, A, B, C, and D were 0.45, 4.0, 2.0, and 0.47 wt %, respectively. This single optimum point for the concentration of the components is in the expected range in the proposed contour plot (Fig. 5). In the optimization plot, it is to be noted that composite desirability (CD) evaluates how the settings optimize a set of responses overall, and assess how well a combination of input variables satisfies the goal. Individual desirability (Id) evaluates how the settings optimize a single response. Here, the composite desirability as well as individual desirability is equal to 1, which indicates that the settings appear to achieve favorable results for all responses as a whole.

Molecular imprinting of verapamil

At the first step, NIP with the optimized composition, i.e., monomer 0.45 wt %, crosslinker 4 wt %, modifier 0.47 wt %, and initiator 2 wt %, was synthesized.

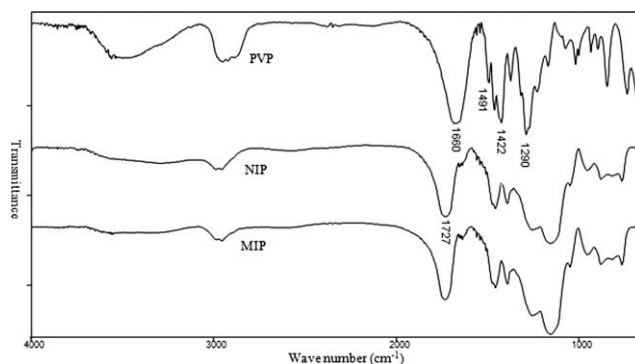


Figure 8 FTIR spectra of MIP, NIP, and PVP.

At the second step, corresponding MIP with verapamil as the template molecule was also prepared. Figure 7 shows SEM image of the resultant particles for NIP/MIP. The weight average particle size obtained from SEM image for NIP was 489 nm. This value is in agreement with the model prediction with about 2% deviation in the particle size. Additionally, the average particle size for the corresponding MIP was found to be about 550 nm. This indicates that imprinting verapamil in poly(AAm-co-MBA) results in the increase of the particle size which is consistent with literature reports.^{22,33} Possibly, in the MIP, additional molecular interaction between the monomer and the template affects the polymer nucleation and consequently results in slightly larger particles.

Figure 8 shows the FTIR spectrum of PVP, MIP, and NIP. The characteristic absorption bands at the frequencies 1660 cm^{-1} (C=O), 1422 cm^{-1} (δCH_2), 1290 cm^{-1} (C–N) are clearly observed for PVP. Meanwhile, the FTIR spectra of the MIP and NIP do not show such characteristic peaks justifying the absence of the modifier molecule in the system. Additionally, the characteristic peaks of the NIP and MIP are almost similar. These observations suggest that the template in MIP and modifier in MIP/NIP have been successfully removed during washing.

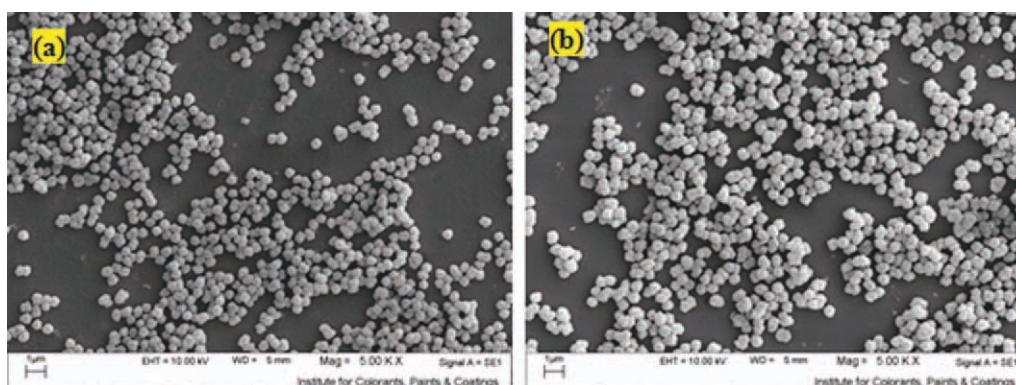


Figure 7 SEM microphotographs of the resultant particles for NIP (a) and MIP (b). [Color figure can be viewed in the online issue, which is available at wileyonlinelibrary.com.]

TABLE V
Elemental Analysis of MIP, NIP, and Theoretical Values

Sample	% C	% H	% N	C/N
MIP	50.40	8.18	16.97	2.97
NIP	50.77	8.65	17.05	2.98
Theoretical ^a	54.14	6.59	18.33	2.95

^a Calculated by eq. (4).

The elemental analysis was performed on the polymers after template extraction indicate that the monomer conversion is high and the monomer has been stoichiometrically incorporated into the polymers (Table V). It is also found that the template has been successfully removed from the polymer. Even though the elemental analysis values for C, H, and N differ from calculated ones, the C/N for both polymers, i.e., MIP and NIP are close to the theoretical values.

DSC analysis of NIP, physical mixture of NIP and verapamil, and verapamil rebind MIP are presented in Figure 9. A small endothermic peak in the physical mixture of NIP and verapamil thermogram (at 149°C, ΔH 9.3 J/g) can be attributed to the template. However, the absence of the crystalline peak of verapamil in the thermogram of the MIP indicates that verapamil and polymer have interacted at molecular level.³⁴

Nitrogen gas sorption isotherms and the pore properties of the MIP and NIP are given in Figure 10 and Table VI, respectively. It is verified that the MIP presents slightly higher surface area than the corresponding NIP. There is a slight difference in the pore volume and surface area of the MIP and NIP as well, which can be attributed to the template effect on the polymer texture.³⁵ Moreover, according to BDDT (Brunauer, Deming, Deming, and Teller)³⁶ isotherm classification, the resultant isotherm shows that the particles are macroporous. The crystallographic data³⁷ have shown that the molecular

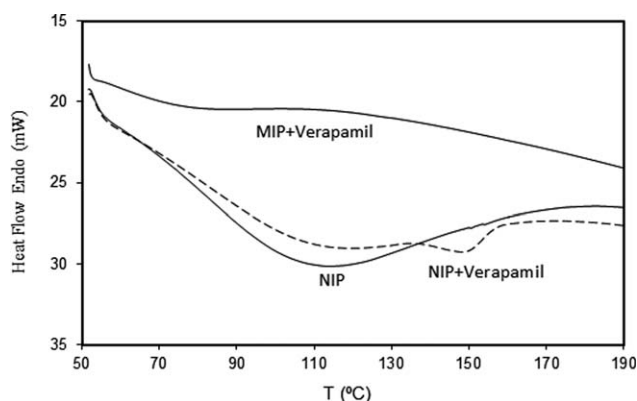


Figure 9 DSC thermograms of NIP, physical mixture of NIP, and verapamil and verapamil-rebind MIP.

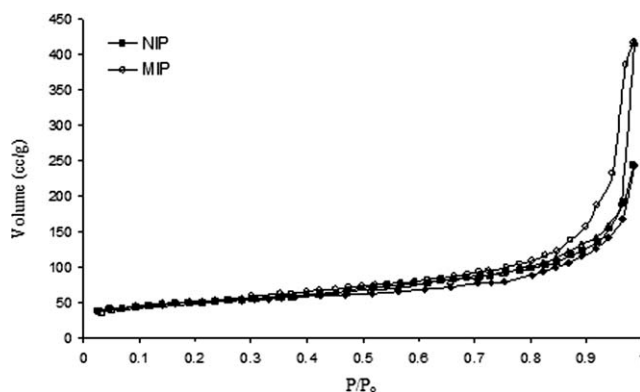


Figure 10 Nitrogen gas adsorption and desorption isotherms for the MIP and NIP.

volume of verapamil in solid-state-conformation is 1382.1 Å³ and the distance between the aromatic rings is 5.25 Å, ($a = 7.086$, $b = 10.591$, $c = 19.196$ Å). Therefore, the macroporous structure of the polymers provides enough big pores for the template to penetrate into the polymer matrix.

Swelling ratios of the MIP and NIP were found to be 1.27 and 1.24, respectively. The swelling ratio values can be regarded as indications of the extent of the cross-linking of the polymeric particles. Since the swelling ratio is not high (for both NIP and MIP), it is inferred that sufficient level of cross-linking has been achieved. Additionally, as the swelling ratios of NIP and MIP show almost similar values, it is deduced that the verapamil imprinting has not influenced the swelling ratio.

Distribution coefficient (K_D), adsorption amount (Q), and molecular imprinting factor (IF) was calculated to evaluate the imprinting effect on verapamil adsorption. The distribution coefficient, according to the classical adsorption model, is expressed as²⁶:

$$K_D = \frac{C_b}{C_f} \quad (9)$$

where C_b and C_f are the concentration of verapamil on the MIP particles ($\mu\text{mol/g}$) and in the solution ($\mu\text{mol/mL}$) at equilibrium, respectively. The concentration of free verapamil was determined by analyzing the supernatant solutions. Using a standard

TABLE VI
Pore Properties of the MIP and NIP

Sample	Surface area (m ² /g)	Pore volume (cc/g)	Pore ratio ^a	Pore size (nm)	
				Meso	Ave. pore size ^b
MIP	186.0	0.647	1.03	3.72	13.91
NIP	168.2	0.625		3.71	14.88

^a The ratio between the pore volumes.

^b Calculated using eq. (5).

calibration curve, the amount of verapamil bound to the polymers was calculated by subtracting the free amount verapamil from the initial amount of that.

As mentioned above the polymers swell very little, therefore, the effect of swelling on the template concentration might be negligible and the amount of verapamil adsorbed by the polymeric particles could be determined by the following equation:

$$Q = \frac{(C_0 - C_f)V}{m} \quad (10)$$

where Q is the mass (mg) of verapamil adsorbed per gram of dry polymer, C_0 (mg/mL) and C_f (mg/mL) are the initial and final verapamil concentration in the supernatant, respectively. V (mL) is the total volume of the verapamil solution, and m is the mass (g) of polymer in rebinding mixture.

The IF was achieved via the following equation:

$$IF = \frac{Q_{MIP}}{Q_{NIP}} \quad (11)$$

where Q_{MIP} and Q_{NIP} are the amount of verapamil adsorbed into a unit mass of dry MIP and NIP at equilibrium, respectively. It is to be noted that the UV absorbance of MeCN solution which had already been equilibrated with the polymers (i.e., gently shaken for 24 h) was the same as that for the neat MeCN. Therefore one could say that the polymers were free from any unreacted materials and no chemicals released from the polymers to disturb the UV absorption. Hence the washing step with MeOH/AcOH and centrifugation were quite sufficient. Otherwise, one needed to assess the background absorbance from any template or oligomers that could desorb from the particles.

In the batch binding assay, verapamil concentration in the supernatants solution of MIP and NIP was measured as 3.17 and 6.86 mM, respectively. Therefore, K_D for the MIP was 21.5 mL/g and the IF was 2.17. The result indicates that the imprinting method creates a microenvironment and nano-cavities including functional groups that recognize verapamil as imprinted molecule. Therefore, verapamil is taken up much more by the MIP than by the NIP. It is noteworthy to mention that verapamil molecule is bearing 6 hydrogen-bond acceptor moieties and the most susceptible group to be hydrogen-bond is the $-C\equiv N$ group in verapamil.³⁷ Therefore, it is hypothesized that the success of the MIP is due to a large number of weak hydrogen bonds formed between the polymer and the template, giving an overall strong interaction.

CONCLUSION

Modified precipitation polymerization method was utilized to obtain poly(AAm-co-MBA) particles with

tunable particle size. This polymerization method involves both precipitation and dispersion polymerization recipes. The Taguchi method for the design of experiment was used to investigate the influence of polymerization constituents, including monomer, crosslinker, initiator, and modifier, on the particle size. Depending on the composition, products with different submicro-particles with sizes ranging between 100 and 600 nm were achieved. In all cases, PDI of the particle size was found to be almost 1 indicating uniformity of the particle size. The crosslinker was found to be the major factor affecting the particles size, even though the initiator and modifier showed also some contribution. It was revealed that the particle size increases by increasing the concentration of the crosslinker. The influence of modifier on the particle size was attributed to the nucleating role of this component. For a predefined particle size, the optimum composition was predicted by Taguchi method. The particle size of the predicted composition for NIP was found to be consistent with the experimentally determined particle size using the SEM. Single point batch rebinding experiment showed the affinity of verapamil as a template to the imprinted polymer. The MIPs especially with a controlled particle size have a potential use for the separation, drug delivery systems, and etc.

References

1. Bene, M. J.; sbreve; Horak, D.; Svec, F. *J Sep Sci* 2005, 28, 1855.
2. Swadesh, J. *HPLC: Practical and Industrial Applications*; CRC Press: Boca Raton, 1997.
3. Mayes, A. G.; Mosbach, K. *Anal Chem* 1996, 68, 3769.
4. Vaihinger, D.; Landfester, K.; Kräuter, I.; Brunner, H.; Tovar, G. E. M. *Macromol Chem Phys* 2002, 203, 1965.
5. Sellergren, B. *Anal Chem* 1994, 66, 1578.
6. Wang, J.; Cormack, P. A. G.; Sherrington, D. C.; Khoshdel, E. *Angew Chem* 2003, 115, 5494.
7. Kubo, T.; Hosoya, K.; Watabe, Y.; Ikegami, T.; Tanaka, N.; Sano, T.; Kaya, K. *J Chromatogr A* 2003, 987, 389.
8. Komiyama, M.; Takeuchi, T.; Mukawa, T.; Asanuma, H. *Molecular Imprinting: From Fundamentals to Applications*; Wiley-VCH, Verlag GmbH, 2003.
9. Sellergren, B. *Molecularly Imprinted Polymers: Man-Made Mimics of Antibodies and Their Applications in Analytical Chemistry*; Elsevier: Amsterdam, 2001.
10. Perez-Moral, N.; Mayes, A. G. *Anal Chim Acta* 2004, 504, 15.
11. Liu, H.; Row, K. H.; Yang, G. *Chromatographia* 2005, 61, 429.
12. Arshady, R. *Colloid Polym Sci* 1992, 270, 717.
13. Jin, Y.; Jiang, M.; Shi, Y.; Lin, Y.; Peng, Y.; Dai, K.; Lu, B. *Anal Chim Acta* 2008, 612, 105.
14. Horváth, V.; Lorántfy, B.; Tóth, B.; Bognár, J.; László, K.; Horvai, G. *J Sep Sci* 2009, 32, 3347.
15. Nematollahzadeh, A.; Sun, W.; Aureliano, C. S. A.; Lütkenmeyer, D.; Stute, J.; Abdekhodaie, M. J.; Shojaei, A.; Sellergren, B. *Angew Chem Int Ed Engl* 2011, 50, 495.
16. Brogden, R. N.; Benfield, P. *Drugs* 1996, 51, 792.
17. Mullett, W. M.; Wallis, M.; Levsen, K.; Borlak, J.; Pawliszyn, J. *J Chromatogr B* 2004, 801, 297.
18. Javanbakht, M.; Shaabani, N.; Abdouss, M.; Ganjali, M. R.; Mohammadi, A.; Norouzi, P. *Curr Pharm Anal* 2009, 5, 269.

19. Roy, R. K. *A Primer on the Taguchi Method*; Society of Manufacturing Engineers: New York, 1990.
20. Abramoff, M. D.; Magelhaes, P. J.; Ram, S. J. *Biophoton Int* 2004, 11, 36.
21. Ignac, C.; Medyan, R.; Mitsuru, A. *Die Makromol Chem* 1992, 193, 2843.
22. Pan, G.; Zu, B.; Guo, X.; Zhang, Y.; Li, C.; Zhang, H. *Polymer* 2009, 50, 2819.
23. Wheeler, A.; Frankenburg, W. G.; Komarewsky, V. I.; Rideal, E. K.; Emmett, P. H.; Taylor, H. S. *Advances in Catalysis*; Academic Press, New York, 1951.
24. Sellergren, B.; Ekberg, B.; Mosbach, K. *J Chromatogr A* 1985, 347, 1.
25. Chen, Z.; Hua, Z.; Xu, L.; Huang, Y.; Zhao, M.; Li, Y. *J Mol Recognit* 2008, 21, 71.
26. Yan, M. *Molecularly Imprinted Materials: Science and Technology*; Marcel Dekker: New York, 2005.
27. Spizzirri, U. G.; Peppas, N. A. *Chem Mater* 2005, 17, 6719.
28. Downey, J. S.; Frank, R. S.; Li, W.-H.; Stover, H. D. H. *Macromolecules* 1999, 32, 2838.
29. Blackley, D. C., Ed. *Polymer Latices: Types of Latices*; Springer-Verlag: New York, LLC, 1997.
30. Hiroshi, A. *ACM Trans Math Softw* 1978, 4, 148.
31. Cooke, R.; Mostaghimi, S.; Parker, J. C. *Environ Monit Assess* 1993, 28, 33.
32. Ishihara, M. *Int J Comput Sci Netw Security* 2006, 6, 205.
33. Yoshimatsu, K.; LeJeune, J.; Spivak, D. A.; Ye, L. *Analyst (Cambridge, U. K.)* 2009, 134, 719.
34. Horoz, B. B.; Kılıçarslan, M.; Yüksel, N.; Baykara, T. *AAPS PharmSciTech* 2006, 7, E1.
35. Urraca, J. L.; Carbajo, M. C.; Torralvo, M. J.; Gonzalez-Vazquez, J.; Orellana, G.; Moreno-Bondi, M. C. *Biosens Bioelectron* 2008, 24, 155.
36. Brunauer, S.; Deming, L. S.; Deming, W. E.; Teller, E. *J Am Chem Soc* 1940, 62, 1723.
37. Carpy, A.; Leger, J.-M.; Melchiorre, C. *Acta Crystallogr Sect C* 1985, 41, 624.